

# Compartmental model of $^{18}\text{F}$ -choline

T Janzen<sup>\*1</sup>, F Tavola<sup>2</sup>, A Giussani<sup>1</sup>, MC Cantone<sup>2</sup>, H Uusijärvi<sup>3</sup>, S Mattsson<sup>3</sup>, M Zankl<sup>1</sup>, N Petoussi-Henß<sup>1</sup> and C Hoeschen<sup>1</sup>

<sup>1</sup>Institute of Radiation Protection, Helmholtz Zentrum München, Neuherberg, Germany

<sup>2</sup>Università degli Studi di Milano, Milano, Italy

<sup>3</sup>Medical Radiation Physics, Lund University, Malmö University Hospital, Malmö, Sweden

## Abstract

The MADEIRA Project (Minimizing Activity and Dose with Enhanced Image quality by Radiopharmaceutical Administrations), aims to improve the efficacy and safety of 3D functional imaging by optimizing, among others, the knowledge of the temporal variation of the radiopharmaceuticals' uptake in and clearance from tumor and healthy tissues. With the help of compartmental modeling it is intended to optimize the time schedule for data collection and improve the evaluation of the organ doses to the patients.

Administration of  $^{18}\text{F}$ -choline to screen for recurrence or the occurrence of metastases in prostate cancer patients is one of the diagnostic applications under consideration in the frame of the project. PET and CT images have been acquired up to four hours after injection of  $^{18}\text{F}$ -choline. Additionally blood and urine samples have been collected and measured in a gamma counter.

The radioactivity concentration in different organs and data of plasma clearance and elimination into urine were used to set-up a compartmental model of the biokinetics of the radiopharmaceutical. It features a central compartment (blood) exchanging with organs. The structure describes explicitly liver, kidneys, spleen, plasma and bladder as separate units with a forcing function approach. The model is presented together with an evaluation of the individual and population kinetic parameters, and a revised time schedule for data collection is proposed. This optimized time schedule will be validated in a further set of patient studies.

**Keywords:**  $^{18}\text{F}$ -choline, PET, model, prostate carcinoma

## 1. Introduction

The European collaborative project MADEIRA (Minimizing Activity and Dose with Enhanced Image quality by Radiopharmaceutical Administrations) aims to improve the efficacy and safety of 3D functional imaging and reduce the radiation exposures of the patients. This goal is achieved by optimizing, among others, the knowledge of the temporal variation of the radiopharmaceuticals' uptake in and clearance from tumor and healthy tissues. Among the tasks are the optimization of image acquisition schedules and the refinement of absorbed dose assessment making use of specific pharmacokinetic models. For the development of the models, biokinetic data such as activity concentrations in different tissues and in the biological fluids of the patients are essential. Administration of  $^{18}\text{F}$ -choline to screen for recurrence or the occurrence of metastases in prostate cancer patients in case of elevated PSA (prostate-specific antigen) levels is one of the diagnostic applications under consideration in the frame of the project.

Choline is a peptide that is necessary for the synthesis of phospholipids, essential parts of every membrane in the human organism. Increased levels of choline and phosphocholine are a widely established characteristic of prostate cancer cells<sup>[1,2]</sup>. This is caused by an overexpression of choline kinase (ChoK) in these cells<sup>[3,4]</sup>. ChoK is responsible for metabolizing choline and part of the pathway of the synthesis of phospholipids for cell membranes. Several studies have investigated the usefulness of Positron Emission Tomography (PET) with  $^{11}\text{C}$ - or  $^{18}\text{F}$ -choline for the diagnosis and

---

\* Presenting author: [tilman.janzen@helmholtz-muenchen.de](mailto:tilman.janzen@helmholtz-muenchen.de)

staging of prostate carcinoma<sup>[5-8]</sup>. The results were encouraging and other studies on the kinetics of choline were conducted. One study investigated the metabolism of choline in blood of humans and mice in the first 40 minutes after injection<sup>[9]</sup>. Other studies included PET scans after administration of radiolabelled choline<sup>[7,8,10,11]</sup>, however no biokinetic data in humans for more than one hour after injection were available up to now.

This study presents the biokinetic model for <sup>18</sup>F-choline derived from patient clinical data (PET/CT images, blood clearance and elimination into urine) collected for up to four hours after administration.

## 2. Materials and Methods

Patient measurements were performed at the Nuclear Medicine Department at the Malmö University Hospital<sup>[12]</sup> according to the protocol approved by the Regional Ethical Vetting Board at Lund University. The <sup>18</sup>F-choline was synthesized at the synchrotron facilities at Lund University Hospital and delivered to Malmö. Six patients suffering from prostate cancer participated in the study. They had previously undergone prostatectomy and a <sup>18</sup>F-choline examination was scheduled to screen for recurrence and the occurrence of metastases after raised PSA levels were detected. Four PET images (thigh to neck) together with two corresponding CT images were acquired with a Philips Gemini PET/CT scanner directly after the injection (administered activity: 4 to 5 MBq per kg body weight) and at 1, 2 and 3 or alternatively 4 hours thereafter. PET scans were attenuation-corrected using the CT images (slice thickness 5mm, voxel size 80mm<sup>3</sup>). Additionally blood and urine samples were collected between the PET scans. In two patients blood samples were taken also before the first PET scan. An idealized timeline for the measurements is shown in Figure 1.

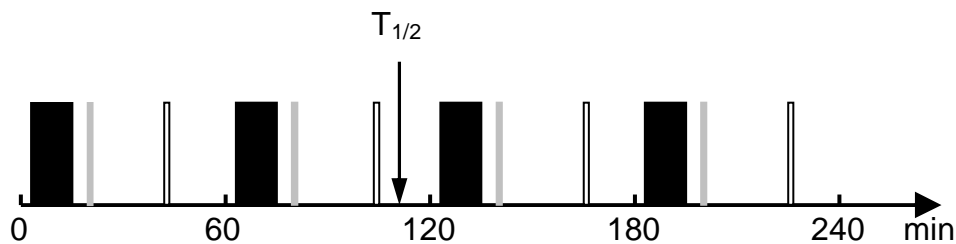


**Figure 1:** Idealized timeline of the measurement protocol. A PET scan (black box) is followed by a blood sample (gray box) and an urine sample (empty box). The half-life ( $T_{1/2}$ ) of <sup>18</sup>F is also indicated.

The activity concentrations in the liver, kidneys, spleen, urinary bladder and, if present, in tumor or metastases were determined using the implemented software tool provided with the scanner (ROIs manually defined). The software assumes constant activity concentration over the duration of one scan (15 - 25 minutes) and internally calculates the activity concentration at the time of the beginning of the scan. However the assumption of constant concentration is not correct for the first scan which takes place immediately after the injection, and thus in a phase where the pharmaceutical is still taken up into the organs. Therefore the automatic calculation performed by the software cannot account for the rapid changes in the activity distribution that take place during the scan. The accuracy of this information is important for the correct development of the biokinetic model; therefore we implemented an algorithm that accounts for the position of each organ and thus refers the measured activity concentration to the exact time point of the measurement for that organ. The activity concentration values were finally transformed into absolute activity values using the organ volumes as determined from the registered CT images.

The blood and urine samples were measured in an automatic gamma counter (WIZARD 1480, Wallace). A correction of the counting efficiency at different activity levels was implemented.

These data on the distribution of the radioactivity in the organs and tissues were used to set up a compartment model of the biokinetics of <sup>18</sup>F-choline. In such a model the system under investigation is represented by several compartments containing the radiopharmaceutical. Connections between the compartments that allow for exchange are described by differential equations. In this modeling process two different software packages were used, SAAM II<sup>®[13]</sup> and ADAPT 5<sup>[14]</sup>, in order to verify the stability of the results depending on the algorithms and on the minimization techniques employed. In SAAM II<sup>®</sup> the optimization is performed by a modified Gauss-Newton method, while the Rosenbrock

integrator is used to solve the differential equations. ADAPT uses the differential equation solver LSODA (Livermore Solver for Ordinary Differential equations with Automatic method switching for stiff and nonstiff problems).

The starting model was structured on the basis of the available data, featuring a central exchange compartment, where the injected radiopharmaceutical is initially distributed, and a series of subsystems representing the organs and tissues which concentrated most of the activity and which were easily imaged in all patients: liver, kidneys, spleen and urinary bladder. For some patients activity concentrations were available also for the salivary glands, tumors and/or metastasis. The activities present in these regions were small, so that at this stage of the analysis it was decided not to indicate them explicitly in the general model structure. A further compartment (Rest of the Body, RoB) was added, to account for the material which is transported to organs and tissues different than those explicitly modeled. Identifiability (the possibility of having unique solutions) of the compartmental system was verified using the GLOBI software<sup>[15]</sup>. The model structure had to be refined to be able to properly describe the experimental data. To this purpose, two alternative approaches were used<sup>[16]</sup>: (i) the introduction of non-linear kinetics (ii) the definition of substructures using the forcing function approach<sup>[17]</sup>. Due to the complexity of the initial model structure, the latter method was considered more reliable.

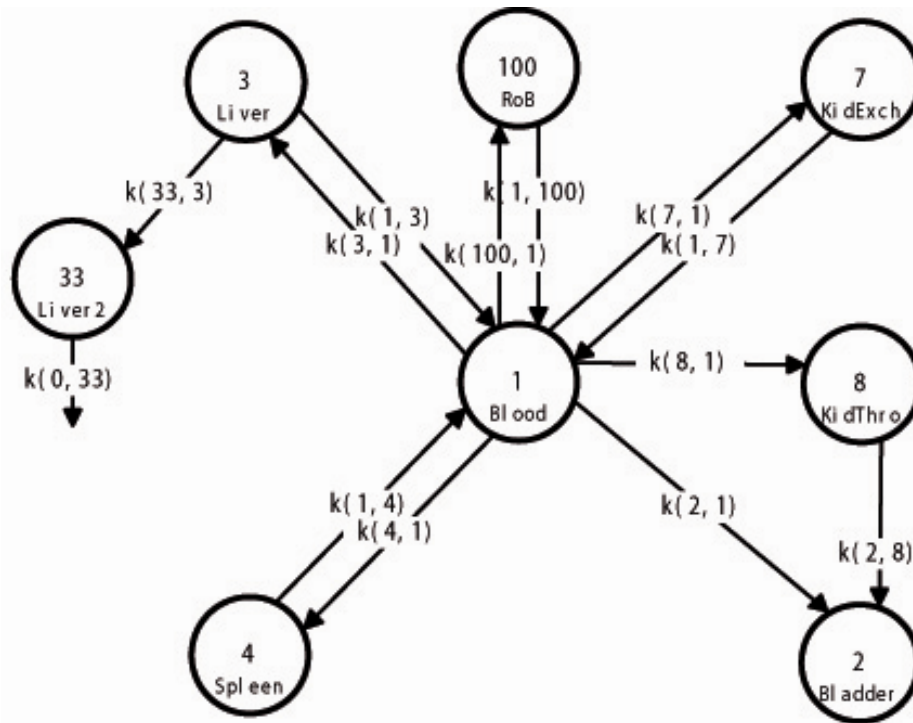


**Figure 2:** The complete model structure

This method allows decoupling a complex multi-compartment model that features a central exchange compartment into several subsystems that are independent of one another. The activity in the central compartment was described with a sum of exponentials with fixed coefficients (forcing function). For each decoupled system, its structure and the parameter values were determined by using the fixed forcing function as an input and fitting the model predictions only to the data collected in that subsystem. The separate substructures were then recombined into the complete model, the forcing function lifted and the new fit performed in the recombined structure. The parameter values obtained in the subsystem analysis were used as starting estimates. Individual patient estimation and population kinetic analysis were performed on the available set of data. With the latter approach the model is fitted to all data of all patients simultaneously. This method, beyond providing the characteristic values of the population means and of the population standard deviations, can make better use of the whole set of data, compensating for partially incomplete individual sets of data. For population kinetics analysis, two of the modules available in ADAPT 5, ITS and MLEM, were used. In MLEM the nonlinear mixed-effects maximum likelihood (ML) problem is solved with the expectation maximization

(EM) algorithm using importance sampling. In the iterative two-stage (ITS) method developed by Prevost, Steimer and Mallet, the Nelder-Mead simplex algorithm is used for minimization purposes.

### 3. Results and Discussion

#### 3.1 The model:

The chosen general model structure as obtained using the forcing function approach is shown in Figure 2. The kidney-bladder subsystem is composed of three compartments according to the description generally used by the ICRP in the biokinetic models for workers and members of the public<sup>[18]</sup>. In the individual fits, bladder voiding was modeled simulating the voiding pattern of each patient. The liver is represented by two compartments. During the forcing function modeling of the liver this proved to give the best fits of the model to the data.

**Table 1:** Parameter values estimated by individual fit

| Parameter                       | Minimum value | Maximum value | Ratio |
|---------------------------------|---------------|---------------|-------|
| Blood - Liver1 k(3,1)           | 1.19E-02      | 2.39E-02      | 2.01  |
| Liver1 - Blood k(1,3)           | 5.83E-03      | 3.06E-02      | 5.25  |
| Liver1 - Liver2 k(33,3)         | 3.50E-03      | 2.29E-02      | 6.54  |
| Blood - Spleen k(4,1)           | 3.36E-04      | 2.11E-03      | 6.28  |
| Spleen - Blood k(1,4)           | 1.97E-03      | 3.52E-02      | 17.9  |
| Blood - Bladder k(2,1)          | 0             | 4.34E-03      | -     |
| Blood - KidneysExchange k(7,1)  | 4.22E-03      | 2.64E-02      | 6.26  |
| KidneysExchange - Blood k(1,7)  | 3.51E-03      | 2.89E-01      | 82.3  |
| Blood - KidneysThrough k(8,1)   | 1.27E-03      | 3.86E-03      | 3.04  |
| KidneysThrough - Bladder k(2,8) | 7.71E-04      | 4.72E-02      | 61.2  |
| Blood - RoB k(100,1)            | 2.86E-02      | 8.09E-02      | 2.83  |
| RoB - Blood k(1,100)            | 1.92E-03      | 7.76E-03      | 4.04  |
| Volume [ml]                     | 5.29E+03      | 3.26E+04      | 6.16  |

Table 1 summarizes the range of the parameter values as obtained in the individual fits. As the excretion into feces, modeled by the exits from blood and from liver2, is slow compared to the measurement time of only four hours after injection, the corresponding parameters were assumed to be zero. It can be seen that there are large variations especially for the parameters describing the return to the circulation k(1,3), k(1,4), k(1,7) and k(1,100) (ratio between maximum and minimum values as high as 80) and those describing the renal excretion(k(8,1), k(2,8) and k(2,1)). These parameters also show high uncertainties with percentage standard deviations ranging from 22 % up to 233 % compared with a median of all parameters of 36 %. This can be explained, among others, with the short duration of the studies in relation to the expected characteristic times of these processes (in the order of a few days) and of the impossibility in some cases to perform the full sampling protocol. For the urinary excretion, the individual collection scheme may also play a role.

The large value of the distribution volume (from 5 to 35 liters) indicates that <sup>18</sup>F-choline is initially distributed also in the interstitial fluids. This parameter was however difficult to estimate with good precision in the individual fits, as in most of the patients the first blood sample was collected only after about 30 minutes.

A better picture can be obtained from the results of the population kinetics analysis, where the model is fitted to all data of all patients simultaneously. Table 2 presents the results of the population analysis using the MLEM estimator, and the corresponding comparisons between experimental data and model curves are given in Figure 3. There is a reasonable agreement for all data sets. It can be observed that activities in liver and spleen have a similar time course, with a decrease corresponding to the physical decay of <sup>18</sup>F, whereas kidneys show a faster uptake and also a fast clearance

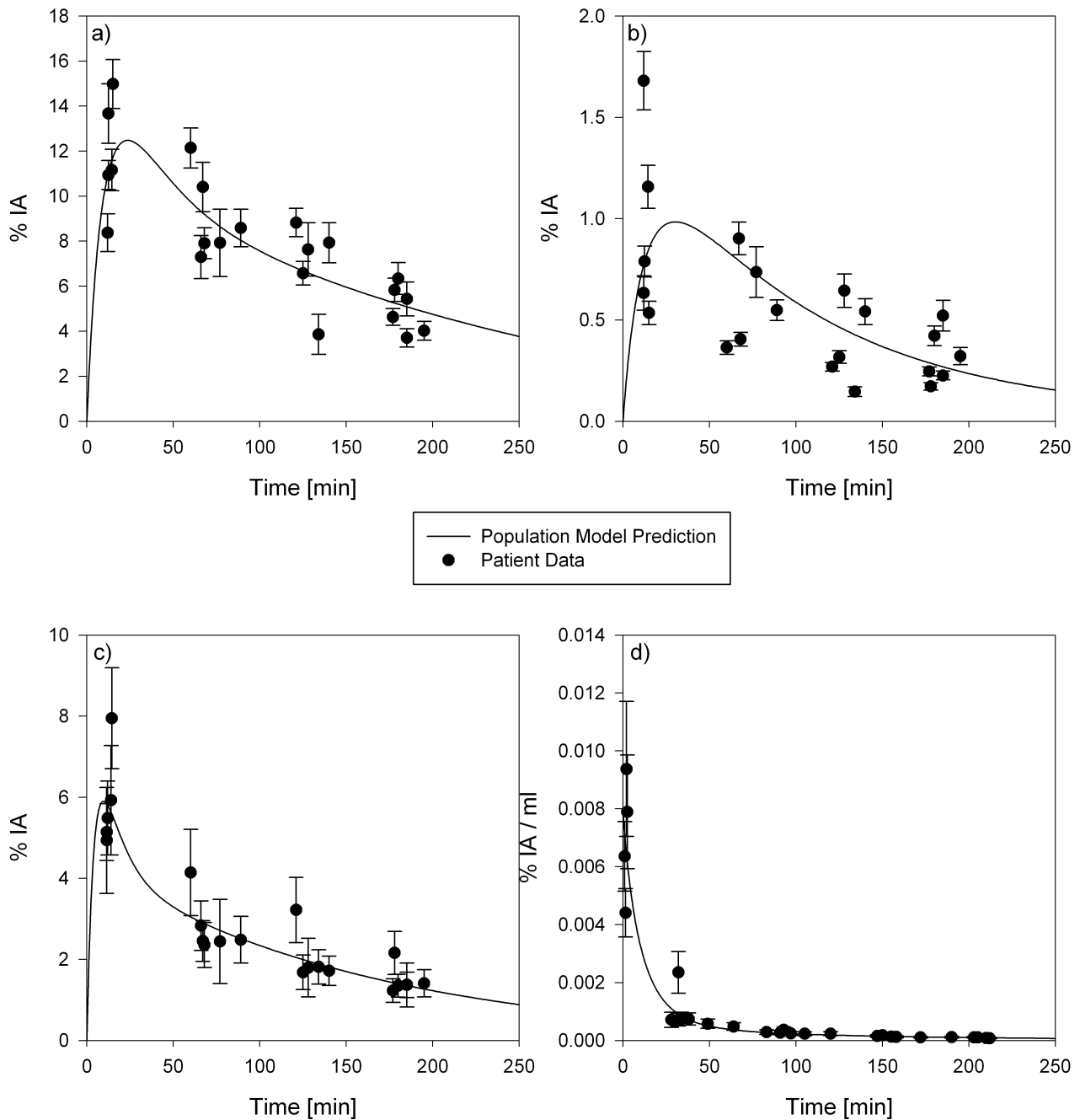


**Figure 3:** Fit of the population model to the patient data given as % of the injected activity (IA): a) Liver; b) Spleen; c) Kidneys; d) Blood

component, ascribable to physiological elimination processes. The coefficients of variation are relatively limited for all parameters (up to a maximum CV% of 42 %), thus indicating that the structure and its parameters give a satisfactory description of the average behavior and no specific individualization is required.

**Table 2:** Parameter values estimated by population analysis

| Parameter                       | Mean     | SD       | SD as CV % |
|---------------------------------|----------|----------|------------|
| Blood - Liver1 k(3,1)           | 1.83E-02 | 2.72E-03 | 14.9       |
| Liver1 - Blood k(1,3)           | 2.50E-02 | 5.54E-03 | 22.1       |
| Liver1 - Liver2 k(33,3)         | 1.54E-02 | 6.37E-03 | 41.5       |
| Blood - Spleen k(4,1)           | 1.18E-03 | 4.92E-04 | 41.6       |
| Spleen - Blood k(1,4)           | 8.74E-03 | 3.56E-03 | 40.8       |
| Blood - Bladder k(2,1)          | 2.64E-03 | 9.79E-04 | 37.1       |
| Blood - KidneysExchange k(7,1)  | 1.66E-02 | 5.45E-03 | 32.8       |
| KidneysExchange - Blood k(1,7)  | 0.191    | 6.29E-02 | 33         |
| Blood - KidneysThrough k(8,1)   | 2.90E-03 | 5.29E-04 | 18.3       |
| KidneysThrough - Bladder k(2,8) | 3.45E-03 | 1.42E-03 | 41.2       |
| Blood - RoB k(100,1)            | 5.51E-02 | 4.54E-03 | 8.24       |
| RoB - Blood k(1,100)            | 4.49E-03 | 1.40E-03 | 31.2       |
| Volume [ml]                     | 1.27E+04 | 4.44E+03 | 35         |

### 3.2 Organ Dose Evaluation:

The developed model and the parameter values resulting from the population analysis were used to evaluate the organ dose received by a standard patient during a  $^{18}\text{F}$ -choline study. The values are presented in Table 3. In comparison the values presented by Noßke and Brix<sup>[19]</sup> are listed. These values were derived from a model based on the biodistribution data of  $^{11}\text{C}$ - and  $^{18}\text{F}$ -choline in animals and humans assuming an infinite biological retention of the activity in organs, as suggested by data in mice. The study presented here has shown that the clearance from kidneys in humans is faster than the physical decay. This may explain why our dose estimate for that organ is lower than that of Noßke and Brix. The lower value for the bladder depends on two factors. One reason is that we assume hourly voiding as in the protocol followed by our patients while Noßke and Brix assume 3.5 hour voiding intervals as in the dynamic kidney-bladder model of the ICRP Publication 53<sup>[20]</sup>. This is reflected by the lower value of the time integrated activity coefficient found in our work. A second reason is that the dose was calculated with the S-factors obtained with adult reference computational phantoms recently adopted by ICRP<sup>[21]</sup>. They give a more realistic (lower) evaluation of the absorption in bladder wall of the beta radiation emitted by the activity in bladder content than the previous mathematical MIRD phantoms used by Noßke and Brix.

**Table 3:** Time-integrated activity coefficients and dose coefficients

| Time-integrated activity coefficients [h] |           |                                | Dose coefficients [mGy/MBq] |           |                                |
|---|-----------|--------------------------------|-----------------------------|-----------|--------------------------------|
| Organ                                     | This work | Noßke and Brix <sup>[19]</sup> | Organ                       | This work | Noßke and Brix <sup>[19]</sup> |
| Liver                                     | 0.410     | 0.37                           | Liver                       | 0.059     | 0.051                          |
| Kidneys                                   | 0.120     | 0.24                           | Kidneys                     | 0.080     | 0.15                           |
| Spleen                                    | 0.024     | 0.053                          | Spleen                      | 0.038     | 0.063                          |
| Bladder contents                          | 0.043     | 0.078                          | Bladder wall                | 0.018     | 0.047                          |
| Other tissues                             | 1.914     | 1.87                           | Other tissues               | ≤ 0.03    | ≤ 0.02                         |

### 3.3 Measurement Protocol Optimization:

As the main purpose of  $^{18}\text{F}$ -choline examinations is the detection of tumors, metastases and recurrences (summarily addressed as lesions), optimization of the imaging procedure means optimizing the visibility of the lesions. Therefore we

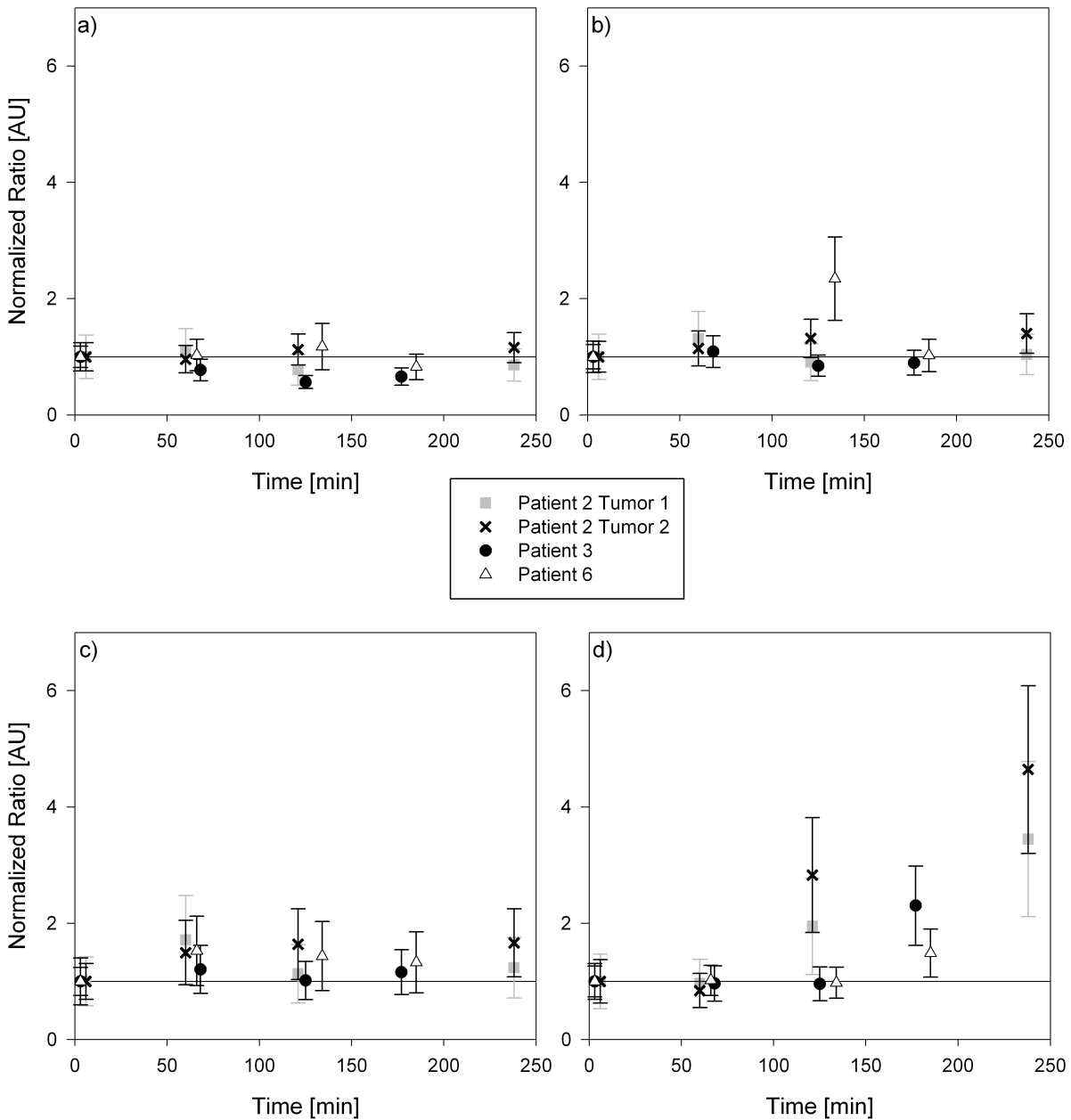


**Figure 4:** The time development of the ratio of the activity concentration in the lesion and in selected organs, normalized to the first time point. a) Liver; b) Spleen; c) Kidneys; d) Bladder.

compared the activity concentrations in lesions and in several organs measured in the same PET scan for the three patients for whom lesions had been imaged (Figure 4). The concentration ratios were normalized to the ratio at the first time point to visualize its time development. For the assessment we assume that a higher ratio means a better contrast between lesion and organ. In liver and spleen the ratio kept a constant level around 1, because in these organs, as in the lesion, there is almost no biological clearance but only physical decay. For kidneys, the normalized ratio is systematically larger than 1 for  $t > 1$  h. This can be explained with the initial rapid decrease observed in the kidneys. Due to the magnitude of the associated uncertainties and the limited number of patients, however, the significance of this trend is questionable. More evident is the increasing trend observed for the ratio lesion to bladder. In this case, there is a rapid uptake of the radiopharmaceutical into the bladder, shortly after the administration, but the material is fully

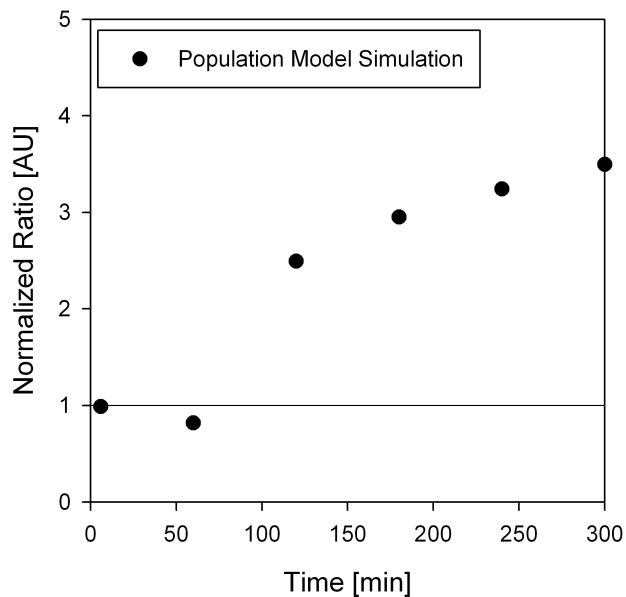


**Figure 5:** Ratio of the activity concentrations in lesion and bladder simulated with the population model.

eliminated relatively frequently since the patients are asked to empty their bladder before the subsequent scan. This creates a favorable condition for the detection of the lesions in the region near or around the bladder, and additionally reduces the doses to this organ. To characterize this further, use was made of the developed model structure. A simulation was performed, assuming fast uptake and infinite retention for the lesion, uptake into the bladder according to the results of the population model, and a voiding interval of 60 minutes. Figure 5 shows the ratio of the activity in the lesion and the activity in the bladder immediately before the voiding of the bladder, i.e. the worst possible case. The ratio at 5 minutes after administration was taken as the reference (normalization) ratio. Here again the ratio is increasing after 120 minutes.

This ratio of lesion to bladder is especially interesting as the prostate is situated very close to the bladder. Therefore it is important but sometimes very hard for the radiologist to discriminate between activity in the bladder and uptake in a lesion. Our results are a first hint that at scans later than 60 minutes after administration a lesion in the vicinity of the bladder might be more visible even if the bladder had not been voided previous to the scan.

Earlier studies have remarked on the lack of a systematical evaluation of the optimal timing for prostate PET with  $^{18}\text{F}$ -choline<sup>[7]</sup>. Several protocols like a single phase whole body scan early after injection or 1 hour delayed scan or a dual phase dynamic scan of the pelvis together with a whole body scan have been proposed. The question is whether the imaging can be improved by a potentially increased lesion contrast at later times or if artifacts by bladder activity and the short half-life make the detection of lesions at later times more difficult. Because our study included information on the biokinetics of  $^{18}\text{F}$ -choline beyond 1 hour after administration, we have found that accumulated activity in the bladder at time points later than 60 min after administration is not impairing the visibility of lesions. Also Kwee et al.<sup>[7]</sup> and Steiner et al.<sup>[8]</sup>, on the basis of different considerations, had shown that imaging at 1 hour after administration or later is important for the detection of malignant lesions and their discrimination from benign ones.

#### 4. Conclusions and Outlook

Our results indicate that PET scans later than 1 hour after injection of  $^{18}\text{F}$ -choline have the potential to improve the detection of malignant lesions during diagnostic examinations. In case of biokinetic investigations, the measurement scheme should be altered with regard to the blood sampling, as an early blood sample before the first PET scan can

reduce the uncertainty in the estimate of the volume of distribution. As our study is based on only six patients with partially incomplete data sets our findings will have to be validated in a larger population of patients. It is intended to include tumor explicitly in the model and to perform a systematic evaluation of the activity concentration in the regions immediately surrounding the detected lesions.

### Acknowledgements

The work was carried out within the Collaborative Project "MADEIRA" ([www.madeira-project.eu](http://www.madeira-project.eu)), cofunded by the European Commission through EURATOM Seventh Framework Programme (Grant Agreement FP7-212100).

### References

1. Ackerstaff, E., et al. "Detection of increased choline compounds with proton nuclear magnetic resonance spectroscopy subsequent to malignant transformation of human prostatic epithelial cells." *Cancer Res.* 61, 3599–3603 (2001).
2. Ackerstaff, E., et al. "Choline phospholipid metabolism: a target in cancer cells?" *J Cell Biochem.* 90, 525–33 (2003).
3. Macara, I.G., "Elevated phosphocholine concentration in ras-transformed NIH3T3 cells arises from increased choline kinase activity, not from phosphatidylcholine breakdown." *Mol Cell Biol.* 9, 325–328 (1989).
4. Ramirez de Molina, A., et al. "Overexpression of choline kinase is a frequent feature in human tumor-derived cell lines and in lung, prostate, and colorectal human cancers." *Biochem Biophys Res Commun.* 296, 580–583 (2002).
5. DeGrado, T.R., et al. "Synthesis and evaluation of  $^{18}\text{F}$  labeled choline as an oncologic tracer for positron emission tomography: initial findings in prostate cancer." *Cancer Res.* 61, 110–117 (2000).
6. Husarik, D.B., et al. "Evaluation of [(18F)-choline PET/CT for staging and restaging of prostate cancer." *Eur J Nucl Med Mol Imaging.* 35, 253–263 (2008).
7. Kwee, S.A., et al. "Localization of primary prostate cancer with dual-phase  $^{18}\text{F}$ -fluorocholine PET." *J Nucl Med.* 47, 262–269 (2006).
8. Steiner, C., et al. "Three-phase  $^{18}\text{F}$ -fluorocholine PET/CT in the evaluation of prostate cancer recurrence." *Nuklearmedizin.* 48, 1–9 (2009).
9. Roivainen, A., et al. "Blood metabolism of [methyl- $^{11}\text{C}$ ] choline: implications for in vivo imaging with positron emission tomography." *Eur J Nucl Med.* 27, 25–32 (2000).
10. DeGrado, T.R., et al. "Pharmacokinetics and Radiation Dosimetry of  $^{18}\text{F}$ -Fluorocholine" *J Nucl Med.* 43, 92–96 (2002).
11. Sutinen, E., et al. "Kinetics of [ $^{11}\text{C}$ ] choline uptake in prostate cancer: a PET study." *Eur J Nucl Med Mol Imaging.* 31, 317–324 (2004).
12. Uusijärvi, H., et al. "Biokinetics of  $^{18}\text{F}$ -choline studied in four prostate cancer patients" Accepted for publication in *Rad Prot Dos.* (2010).
13. Barrett, P.H.R., et al. "SAAM II: Simulation, analysis, and modeling software for tracer and pharmacokinetic studies" *Metabolism.* 47(4), 484–492 (1998).
14. D'Argenio, D.Z., Schumitzky, A. and Wang, X., "ADAPT 5 User's Guide: Pharmacokinetic/Pharmacodynamic Systems Analysis Software." Biomedical Simulations Resource, Los Angeles, (2009).
15. Audoly, S., et al. "Global identifiability of linear compartment models. A computer algebra algorithm." *IEEE Trans. Biom. Eng.* 4, 36–47 (1998).
16. Janzen, T., et al. "Preliminary compartmental model of  $^{18}\text{F}$ -choline" Third Malmö Conference on Medical Imaging (2009).
17. Foster, D.M., "Developing and testing integrated multicompartment models to describe a single-input multiple-output study using the SAAM II software system", [Clifford ed. "Mathematical Modeling of Experimental Nutrition"] Plenum Press, New York, 59–78, (1998).
18. ICRP Publication 67. *Annals of the ICRP* 23(3–4), (1993).
19. Noßke, D., Brix, G., "Dose assessment for C-11- and F-18-choline" SNM Annual Meeting, Toronto (2009).
20. ICRP Publication 53. *Annals of the ICRP* 18(1–4), (1987).
21. ICRP Publication 100. *Annals of the ICRP* 39(2), (2009).